Virtual Sensors for Diagnosis and Prognosis Purposes in the Context of Elastic Mechanical Structures

Frank Heidtmann, Dirk Söffker

***Abstract*—This contribution deals with a model-based approach for diagnosis and prognosis tasks in the context of elastic mechanical structures in conjunction with the *Safety and Reliability Control Engineering* (SRCE) concept. In elastic mechanical structures faults are given by structural changes in mass and/or stiffness, caused by cracks, lost of material or for example by the internal delamination processes of carbon fiber laminate materials. The latter affects modern light weighted structures which are more and more used for example in aircraft constructions. Especially for such safety-critical systems, online and in-situ fault diagnosis are desired. Structural-Health-Monitoring (SHM) concepts deal with different tools to realize safe systems, applying fault monitoring and repair mechanism in combination with approaches for monitoring the hazard rate of complete complex systems.**

The contribution provides new results for the application of the Proportional-Integral-Observer (PIO) for the fault localization in elastic mechanical systems. At this the PIO works as a virtual sensor. Moreover the PIO can be applied for fault detection and estimation. Therewith it can provide inputs for the SRCE concept. That one gives a framework and strategy to calculate the actual reliability of a system under operation what may be used for the purpose of predictive/condition-based maintenance in the context of SHM concepts.

I. Introduction

BASICALLY, the observer ability to monitor large systems/structures with a comparatively small number of measurements delivers an interesting approach for practical usage and applications.

In the case of elastic mechanical structures faults are given by structural changes in mass and/or stiffness properties, caused by cracks, lost of material or for example by the internal delamination processes of modern carbon fiber laminate materials. These effects of structural changes can be understood as virtual forces or torques acting on a faultless structure. Regarding the virtual forces/torques as unknown inputs of a known system, these inputs can be detected and estimated by a Proportional-Integral-Observer (PIO). The PIO is a time-domain-based approach providing online monitoring opportunities during nominal system operating conditions, i.e. usually no specific system excitation and no measurement data preprocessing (e.g. FFT) is needed. Observers based on model-less unknown input observations are used and enhanced in the last years. Advanced simulation results are given in [24], [20], [3], experimental results of the PIO for practical applications are given by [21], analytical considerations taking measurement noise and model uncertainties into account are given in [22]. This paper deals with the application of the PIO for the localization of faults in elastic mechanical systems.

The diagnosis of elastic mechanical systems comprises fault detection, isolation/localization, and analysis/estimation. But the remaining question is about the actual reliability and lifetime of the system in the presence of faults. Beyond, it is about exerting influence on a system to affect system reliability and to extend system usability/functionality under given physical restrictions.

The common strategy to design a fault tolerant, robust, and reliable system consists of a structural reliability analysis of a planned system's function design. If faults still occur, with which the cause can not be eliminated by a redesign, a Fault Detection and Isolation (FDI) module may be added to the system [2]. If an occurring fault affects the safety of the system or the user's health, Limp Home Mode (LHM) functionality may be added to the system. Its function is to supply a minimal functionality of the system in the case of faults and subsystem failures. In [5] a new design strategy is proposed which combines methods and procedures of structural reliability analysis, FDI (including observer-based techniques) and LHM techniques to achieve a system with optimal functional and spatial integrated components. One core element is the *Safety and Reliability Control Engineering* concept (SRCE) [4]. The concept enables a used, stressed technical system to run up to a specific lifetime in compliance with a defined failure probability by controlling the increase of the failure probability.

The paper is organized as follows. The (modal) PIO and the corresponding basic equations are presented in section II. The (modal) PIO is extended by an numerical optimization approach which enables the usage of the observer for fault localization purposes, the PI-Observer fault diagnosis concept and the details of the localization approach are discussed in section III. This is followed by section IV which introduces a simple test rig and its modeling. The presented PIO-based localization approach is applied on that test rig, taking two different kinds of faults into account. The corresponding experimental results are presented in section V. Finally the *Safety and Reliability Control Engineering* (SRCE) concept presented in section VI forms the link between the "tool" PIO and SHM/CM concepts. The contribution ends with the conclusions and an outlook in the last section.

Both authors are with the Chair of Dynamics and Control, Engineering Faculty, University of Duisburg-Essen, Germany, e-mail: {frank.heidtmann, soeffker}@uni-due.de

Manuscript received xxxx xx, 2008; revised xxxxxx xx, 2009.

II. Modal Proportional-Integral-Observer (MPIO)

The PIO observer theory is at an advanced stage. The theoretical background is given in [17], [18], [19], [20] while PIO developments over the last years are summarized in [21]. The PIO is a special disturbance observer which is able to estimate system states and unknown inputs based on a given system description. With this in mind, the PIO can be regarded as virtual sensor: If no physical sensor is available for direct measurements, the PIO can provide information on states as well as on inputs.

Coming from a systems MDK-representation including known and unknown/virtual inputs, the PIO is derived in modal form. The modal decoupling gives direct access to the models eigenvectors (mode shapes), its modal mass, damping and stiffness parameters as provided by the used experimental modal analysis system. So also the PIO [17], [19], [20] is derived in modal form.

By introducing the state space vector

$$x(t) = \left[\begin{array}{cc} z(t) & \dot{z}(t) \end{array} \right]^{\mathrm{T}} \tag{1}$$

the model can be represented in state space form

$$\begin{aligned} \dot{x}(t) &= \underbrace{\left[\begin{array}{cc} 0 & I \\ -M_{\mathrm{diag}}^{-1} K_{\mathrm{diag}} & -M_{\mathrm{diag}}^{-1} D_{\mathrm{diag}} \end{array} \right]}_{A} x(t) \\ &\quad + \underbrace{\left[\begin{array}{c} 0 \\ M_{\mathrm{diag}}^{-1} \Psi^{\mathrm{T}} W_1 \end{array} \right]}_{B} u(t) \\ &\quad + \underbrace{\left[\begin{array}{c} 0 \\ M_{\mathrm{diag}}^{-1} \Psi^{\mathrm{T}} W_2 \end{array} \right]}_{N} f(t) \, . \end{aligned} \tag{2}$$

The $\bar{C}$ matrix in the corresponding output equation

$$y(t) = \bar{C} \left[\begin{array}{c} q(t) \\ \dot{q}(t) \end{array} \right] = \underbrace{\bar{C} \left[\begin{array}{cc} \Psi & 0 \\ 0 & \Psi \end{array} \right]}_{C} x(t) \tag{3}$$

depends on the system measurements in physical coordinates $y(t)$. Then

$$\begin{aligned} \left[\begin{array}{c} \dot{\hat{x}}(t) \\ \dot{\hat{f}}(t) \end{array} \right] &= \underbrace{\left[\begin{array}{cc} A & N \\ 0 & 0 \end{array} \right]}_{A_{\mathrm{ext}}} \left[\begin{array}{c} \hat{x}(t) \\ \hat{f}(t) \end{array} \right] + \left[\begin{array}{c} B \\ 0 \end{array} \right] u(t) \\ &\quad + \underbrace{\left[\begin{array}{c} L_1 \\ L_2 \end{array} \right]}_{L} (y(t) - \hat{y}(t)) \, , \end{aligned} \tag{4}$$

$$\hat{y}(t) = \underbrace{\left[\begin{array}{cc} C & 0 \end{array} \right]}_{C_{\mathrm{ext}}} \left[\begin{array}{c} \hat{x}(t) \\ \hat{f}(t) \end{array} \right] \tag{5}$$

gives the corresponding MPIO with the error dynamics

$$\begin{aligned} \left[\begin{array}{c} \dot{e}(t) \\ \dot{f}_{\mathrm{e}}(t) \end{array} \right] &= \underbrace{\left[\begin{array}{cc} A - L_1 C & N \\ -L_2 C & 0 \end{array} \right]}_{A_{\mathrm{ext}} - L C_{\mathrm{ext}}} \left[\begin{array}{c} e(t) \\ f_{\mathrm{e}}(t) \end{array} \right] \\ &\quad + \left[\begin{array}{c} 0 \\ -I \end{array} \right] \dot{f}(t) \end{aligned} \tag{6}$$

of its estimation errors $e(t) = \hat{x}(t) - x(t)$ and $f_e(t) = \hat{f}(t) - f(t)$. For an observable system $(A_{\mathrm{ext}}, C_{\mathrm{ext}})$, suitably chosen observer feedback matrix L and a constant disturbance $f(t) = f = const.$, the observer state vector $\hat{x}(t)$ reconstructs the system states $x(t)$ and the integral feedback $\hat{f}(t)$ represents the unknown/virtual system inputs $f(t)$. For a time-varying input $f(t)$ the precision of the approximations strongly depends on the rate of change of $f(t)$ as can be seen in (6). Additionally, model imprecision and measurement noise will limit the achievable observer precision.

The main task of the MPIO or rather PIO design process is the synthesis of the observer feedback matrix L. The main goal of the observer is the estimation of the system states and of the unknown inputs. Therefore the observer matrix $A_{\mathrm{ext}} - LC_{\mathrm{ext}}$ in (6) has to be asymptotically stable and the effect of $\dot{f}(t)$ on the error dynamics has to be minimized. Up to now only qualitative solutions for choosing L are available, pointing out, that

$$\|L_2\| \gg \|L_1\| \tag{7}$$

leads to useful estimation results [22], [21].

For this contribution the standard LQ approach is applied to design the MPIO feedback matrix — what might lead to unrequested mathematical restrictions for L. However, this approach guarantees the asymptotic stability of the observer matrix. But apart from that, the design problem of the L matrix is shifted to the synthesis problem of the two LQ weighting matrices Q and R.

In [23] the loop transfer recovery (LTR) method is used to synthesize the L matrix. The LTR method also uses the LQ approach to solve the matrix Riccati equation. The results point out that for $R = I$ and a diagonal weighting matrix Q, the Q-elements related to the unknown inputs in the extended state vector $\left[\begin{array}{cc} x(t)^{\mathrm{T}} & f(t)^{\mathrm{T}} \end{array} \right]^{\mathrm{T}}$ have a significant influence on the estimation results. They are to be chosen very large in relation to the other Q-elements in order to achieve good estimation results.

Also the LTR method finally leads to (7). However, questions remain:

- Is there an alternative Q-matrix-design without strong weight on the $f(t)$-related Q-elements?
- Which influence on the estimations is provided by the different elements of Q?
- Obviously the estimation errors $e(t)$ and $f_{\mathrm{e}}(t)$ are coupled, cf. (6). Are good state estimations in the presence of bad estimation(s) of the unknown input(s) possible and vice versa? How good can the estimations of the unknown inputs be tuned by means of state measurements? Are the states sensitive enough?
- In the presence of model imprecision and measurement noise: Can the estimations be improved by weighting specific elements of the Q matrix?

These questions are discussed in detail in [1].

III. PIO-BASED DIAGNOSIS OF ELASTIC MECHANICAL STRUCTURES

To ensure the proper and safe operation of a system, it is necessary to detect and locate occurring system faults. Provided that the fault size, its location and its effect on the system characteristics are known, it is possible to realize cost-saving predictive/condition-based maintenance. Corresponding concepts became generally known as Structural Health Monitoring (SHM) or Condition Monitoring (CM) concepts. To ensure system integrity they deal with different tools aimed at fault (online) monitoring, repair mechanisms, limb home mode etc.

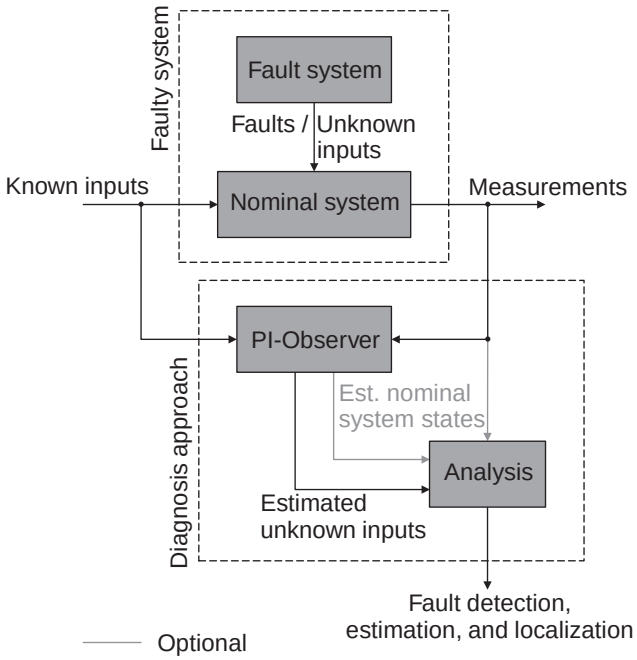

Fig. 1. PI-Observer-based fault diagnosis concept

Figure 1 shows how to apply the PIO for diagnosis purposes. In the case of elastic mechanical structures faults are given by structural changes in mass and/or stiffness properties, caused by cracks, lost of material or for example by the internal delamination processes of modern carbon fiber laminate materials. These effects of structural changes can be understood as virtual forces or torques acting on a faultless structure. Regarding the virtual forces/torques as unknown inputs of a known (nominal) system, these inputs can be detected and estimated (online) by a Proportional-Integral-Observer (PIO) during nominal system operating conditions. For that, the nominal system has to be modeled by a (linear) state space model and the unknown inputs have to be presentable by an additive term, cf. (2). If the necessary observability conditions of the faulty system are fulfilled (i.e. $(A_{\mathrm{ext}}, C_{\mathrm{ext}})$ fully observable, see (6)), the PI-Observer is able to provide an estimation of the unknown inputs as well as of the states of the nominal system. During the faultlessly operation of an observed system no unknown inputs will act and the corresponding PIO estimations are just zero.

That means an occurring fault can be detected and, in addition, the time behavior of the corresponding unknown input is reconstructed. This reconstruction can gain detailed information about the fault by means of a final analysis step concerning fault type and fault cause, if needed in conjunction with the system measurements and estimated system states. For example, in [24] the PIO is used for the crack detection at a rotating shaft and its usage allows the visualization of the crack breathing in detail. Especially the estimation of contact forces can be realized easily by the PIO because no (complex) fault modeling by virtual forces, supposable in the case of cracks, is necessary. For example the detection and contact force estimation of blade rubbing in turbines could be solved by the PIO, cf. [21].

A. PIO for detection and estimation purposes

As stated before the PIO usage requires the modeling of the faults which are to be diagnosed. That means the effects of the faults on the observed structure have to be modeled by virtual forces/torques. How this looks like for the example of a cantilever beam and two different types of faults is illustrated in Fig. 2.

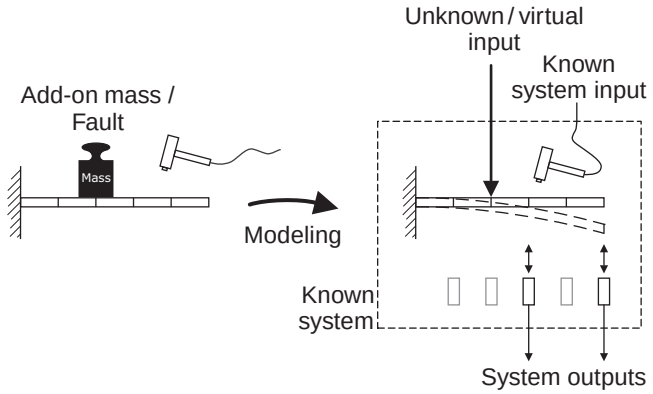

(a) The add-on mass simulates a change in the mass properties of an elastic mechanical system, with it the mass serves as an example of a fault. The fault is understood as realized by a virtual force which can be estimated by the PIO.

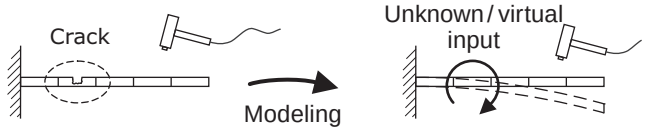

(b) A beam crack is considered. The qualitativ effect of the crack on the beam is modeled by a virtual torque. The torque is the unknown system input which can be estimated by the PIO.

Fig. 2. Faults are understood as virtual forces/torques. They represent the faults and are assumed to act on the undamaged structure. In the form of unknown inputs they can be detected, estimated, and localized by means of the PIO.

In the first case an add-on mass at the beam serves as an example of a fault given by mass accretion/mass lost without changing the stiffness properties of the affected structure significantly. The pictogram on the left-hand side of Fig. 2(a) illustrates the situation - in contrast the real beam introduced later in section IV moves horizontally. The right-hand side of Fig. 2(a) shows the modeling of the fault ”add-on mass”: A single virtual force acts perpendicular to the beam surface and forms the unknown input of a known (nominal/faultless) system. The system is excited by a modal hammer that measures

the contact force - the known input of the system. Furthermore, the beam displacements at one to two positions are used as (known) system outputs - these are the measurements.

In the second case a beam crack is considered, Fig. 2(b). Such a crack mainly affects the beam stiffness without changing its mass properties significantly. In the given case only the beam bending is of interest and its crack-caused changing is modeled by a virtual torque that forms the unknown input of the faultless beam system.

Up to this level it is assumed that the locations of possible faults are known so that the matrix W_2 in (8) and N in (2, 4) respectively is known. If so, the unknown inputs can be detected and estimated. If also the localization of faults is desired additional effort has to be taken into account.

B. PIO for localization purposes

In [22] a set of parallel PIO (observer bank) is used for the localization of the contact point of a beam excitation force. Thereby each observer is related to one possible beam contact point. By the calculation und comparison of the different observer residua the indicating observer and therewith the contact point itself are determined. The results are very sensitive to the time duration of the residua calculation.

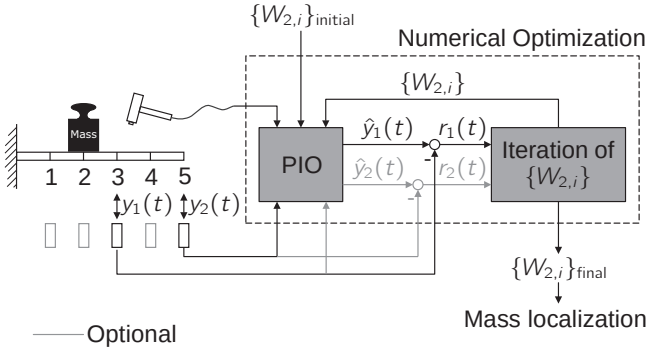

Fig. 3. Numerical Optimization of $W_{2,i}$ by minimization of the residuum r_1

In this contribution the introduced localization approach for changes in the mass properties bases on the optimization of the W_2 matrix and of the N matrix respectively which routes the unknown inputs to the system. Thereby it is assumed that the PIO provides best estimation results if the W_2 matrix denotes the physically correct locations of the unknown inputs/virtual forces. Under this assumption the unknown inputs can be located and estimated.

The system has to be excited by one or more known/measured inputs and at least two system outputs must be available. The system inputs together with one of the system outputs are used to estimate the remaining one (the reference measurement). The resulting error between the estimation and the measurement drives a numerical optimization routine that tunes the W_2 matrix. The finally tuned matrix denotes the searched locations.

For the beam example the measured contact force of the modal hammer gives the system input and the measurements of the two laser sensors the necessary system outputs. The unknown input is given by an add-on mass. It is assumed that the effect of the add-on mass on the beam dynamics can be interpreted as virtual force with unknown time behavior located at the add-on mass position. In the given case W_2 is a vector and its elements correspond to the five beam measurement positions. The largest element of the optimized vector should mark the add-on mass location at the beam. A nonlinear least squares algorithm is used to minimize the sum of squared errors between the PIO-estimations and the reference measurements.

IV. TEST RIG

The following sections present measurements, simulation and optimization results with reference to the beam test rig shown in Fig. 4. Its elastic steel beam of $545 \times 30 \times 5$ mm is clamped onesided. After its short excursion it gets in contact with a heavy steel plate. Thereby the hardness of the contact can be varied by different materials (steel, rubber etc.) of the contact tip at the end of the beam. The arising contact force can be measured by quartz force sensors, which are mounted between the contact plate and ground. Alternatively, the beam can be excited by a modal hammer — the used method for the presented results — which measures the corresponding excitation force. The beam displacements can be determined at two points simultaneously by means of a laser measurement system. Also strain measurements are possible.

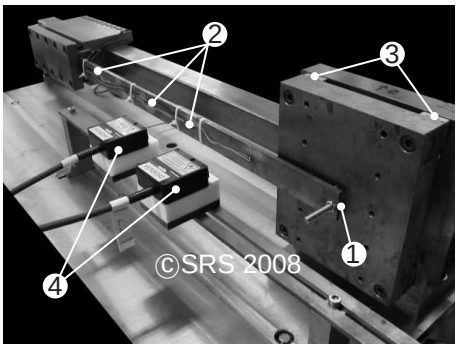

Fig. 4. Beam test rig comprising of a one side clamped elastic beam with (1) contact tip and (2) bonded strain gages, (3) piezo force sensors and (4) laser displacement sensors (SRS, UDuE)

The test rig serves as an example for an elastic mechanical system and is used for research and validation tasks related to the estimation capabilities of the PIO. It provides the possibility to realize short mechanical contacts up to 0.01 seconds like they occur during blade rubbing in rotating machines for example. Other damages in the form of cracks or mass changes can be represented by beam cuts and add-on beam masses.

A. Modeling

Former used theoretically derived finite-element-models have led to increased estimation errors. Thereby it could not be clearly distinguished between the limiting effects of model uncertainties on the one hand and measurement noise on the other. This is based on the fact that measurement noise and model uncertainties cause estimation errors which generally

cannot be quantified. This effect has also been discussed in the previously published papers [25], [26]. So here experimental modeling is applied.

For the localization approach introduced in section III-B the model states have to be in a known relation to at least these different systems DOF in which unknown/virtual inputs might act. One possible approach could be a model updating technique for a theoretically derived finite element model, cf. [11], [12]. This model would provide the necessary mathematical relations and could give feasible model accuracy. However, to meet the requirements and to take only a minimum number of DOF into account, a scaled form of the modal decomposed system description given in (10) is used. The corresponding modal parameters are experimentally determined by means of a modal analysis system. Furthermore, the scaled modal matrix for the transformations between modal and physical coordinates is determined by a sensitivity-based normalization approach, cf. [13], [14], [15]. The resulting model gives the source (initial design) for a final parameter refinement step by parameter estimation in the time-domain to rise model precision.

1) Experimental modeling of elastic mechanical structures: A general linear, time-invariant mechanical system with symmetric mass and stiffness matrices and proportional damping in MDK-representation

$$M\ddot{q}(t) + D\dot{q}(t) + Kq(t) = W_1 u(t) + W_2 f(t) \tag{8}$$

with known inputs $u(t)$ and unknown or virtual inputs $f(t)$ is assumed. The two matrices W_1 and W_2 describe the points of action of the inputs. For linearly independent eigenvectors the system can be modally decomposed by the transformation

$$q(t) = \Psi z(t) \tag{9}$$

using the corresponding modal matrix Ψ and by premultiplying (8) by its transpose. The coupled differential equations are decoupled in that new basis and (8) becomes

$$M_{\mathrm{diag}}\ddot{z}(t)+D_{\mathrm{diag}}\dot{z}(t)+K_{\mathrm{diag}}z(t) = \Psi^{\mathrm{T}}W_1 u(t)+\Psi^{\mathrm{T}}W_2 f(t) \tag{10}$$

with diagonal modal mass matrix M_{diag}, modal damping matrix D_{diag} and modal stiffness matrix K_{diag} in the modal coordinates $z(t)$.

The modal matrix Ψ can be scaled by a scaling vector Υ such that the modal masses become 1 and the modal mass matrix

$$M_{\mathrm{diag}} = (\Upsilon\Psi)^{\mathrm{T}} M (\Upsilon\Psi) = \Phi^{\mathrm{T}} M \Phi = I \tag{11}$$

equals the identity matrix. If so, the modal damping and stiffness matrices are derived to

$$D_{\mathrm{diag}} = [2\omega_k d_k] \quad \text{and} \quad K_{\mathrm{diag}} = [\omega_k^2] \tag{12}$$

with the undamped natural frequency ω_k and the damping ratio d_k of the k^{th} mode. Hence, for known modal parameters and suitably scaled modal matrix Φ the system matrices can be calculated after

$$M = \Phi^{-\mathrm{T}}\Phi^{-1},\ D = \Phi^{-\mathrm{T}}[2\omega_k d_k]\Phi^{-1},\ \text{and}\ K = \Phi^{-\mathrm{T}}[\omega_k^2]\Phi^{-1} \tag{13}$$

or rather the modal model (10) can be set up with Ψ replaced by the scaled matrix Φ.

The needed undamped natural frequencies and damping ratios of the different modes as well as the scaling vector Υ can be experimentally determined. In the case of an output-only modal analysis system a sensitivity-based normalization approach is necessary to get the elements υ_k of the scaling vector [15], [14], [13]:

Let the indices 0 and 1 denote the system before and after a mass change respectively, and let ΔM denote the mass change such that $M + \Delta M$ forms the mass matrix after the mass change. Furthermore assuming no damping or proportional damping and at most small changes in the k^{th} mode shape such that

$$\psi_{k,0} \approx \psi_{k,1} \approx \psi_k \tag{14}$$

holds true, then the corresponding scaling factor is

$$\upsilon_k = \sqrt{\frac{\omega_{k,0}^2 - \omega_{k,1}^2}{\omega_{k,1}^2 \psi_k^{\mathrm{T}} \Delta M \psi_k}}\ . \tag{15}$$

The derived model of course possess exactly the measured natural frequencies, damping ratios and mode shapes. Apart from the scaling vector estimation, this kind of modeling is fast and exact within the scope of measurement precision. Another advantage is that no initial model is needed like for the finite element model updating techniques, cf. [12]. However, if there is a significant mass influence of the modal analysis acceleration sensors on the system dynamics, the derived model has to be refined to meet the pure system dynamics. Details are given in [1].

2) Experimental modeling results: For the experimental modeling the beam is subdivided in five uniform parts as illustrated in Fig. 5. At the positions 1 to 5 acceleration sensors are mounted for the experimental modal analysis. Due to the modeling approach, basically the resulting (initial) model possess exactly the measured modal parameters. In contrast, the underlying assumptions for the identification of the scaling vector cannot be fulfilled exactly, it is always afflicted with inaccuracies due to changes in the mode shapes caused by the necessary mass change. However, the removing of the acceleration sensors breeds the bigger effect. So the (initial) model is refined by a subsequent parameter estimation process due to significant changes in the eigenfrequencies and smaller changes in the mode shapes caused by the (removed) masses of the modal analysis sensors. By this numerical optimization the natural frequencies, damping ratios, and the scaling vector are tuned on the basis of measured excitation force and non-contacting response measurements. Details are given in [16].

The refined initial model, the final model, is validated with the help of measurements of the non-contacting laser sensors: Analogously to the parameter estimation process, the beam is excited by a modal hammer and the resulting beam displacements are measured and compared to corresponding simulations. The results for two different excitation points and measurements in positions 1 to 4 are shown in Fig. 6 to 9.

Figure 6 shows an significant rate of measurement noise due to the small beam displacements close to the clamping position. In Fig. 8 and 9 measurement and simulation results

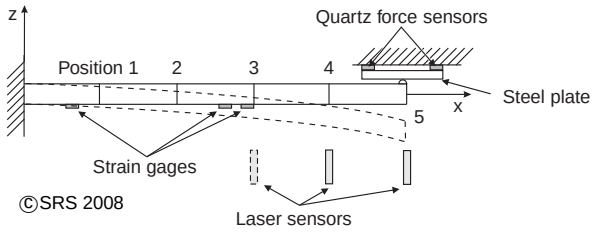

Fig. 5. Test rig sketch illustrating beam subdivision and corresponding measurement positions 1 to 5

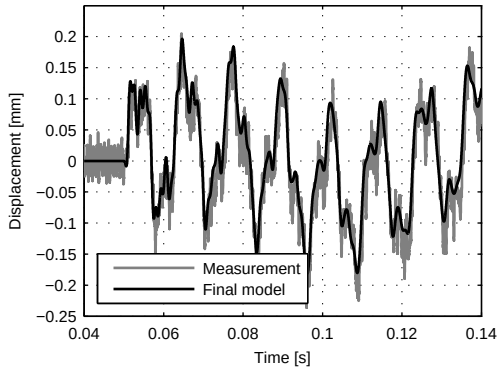

Fig. 6. Model validation for measurement in position 1 and contact in 2

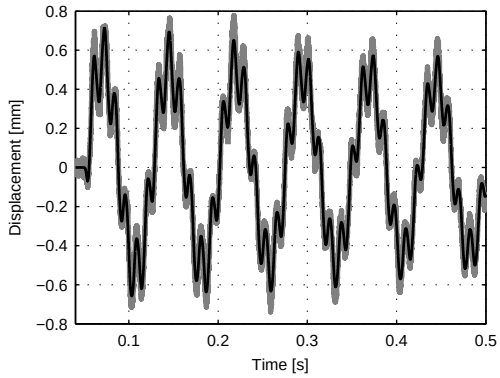

Fig. 7. Model validation for measurement in position 2 and contact in 5

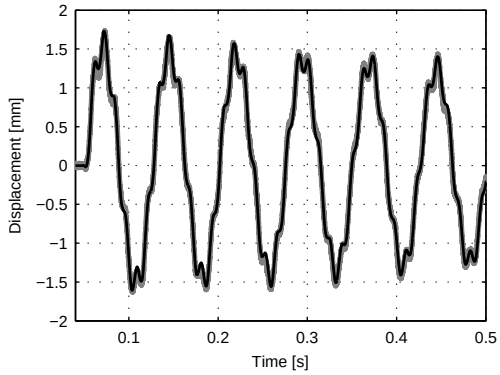

Fig. 8. Model validation for measurement in position 3 and contact in 5

are very similar. However, the measured beam displacements are dominated by the first three beam modes. Also modes 4 and 5 have been included in the initial model, but during the refinement process on the basis of the laser displacement

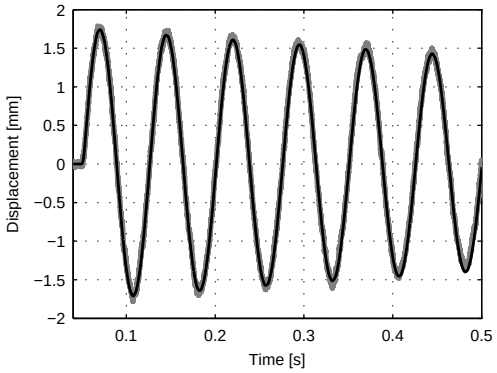

Fig. 9. Model validation for measurement in position 4 and contact in 5

sensors the model cannot be adapted in a reliable way to these modes: The laser measurements do not provide the necessary resolution, the higher modes — naturally coming along with decreasing displacements — are coved by measurement noise. To overcome this difficulty acceleration measurements shall be used, if additional masses can be accepted in case of contacting sensors.

V. Experimental results

The following subsections summarize experimental results for the PIO-based fault localization. At first, results for the localization of beam mass changes are given. As explained above these changes are realized by add-on masses placed upon the cantilever beam. Different masses, measurement and excitation positions are tested. This is followed by experimental results for the localization of a beam crack.

A. Localization of beam mass changes

Figures 10 and 11 show the optimization results of the W_2 vector for different add-on mass locations, excitation and measurement positions. The positions of the different add-on mass locations are marked by circles in the figures. For different tested combinations of measurement and excitation points it is possible to locate masses of about 20 % beam mass with only one displacement measurement as PIO input, see Fig. 10. The localization of masses of about 15 % beam mass

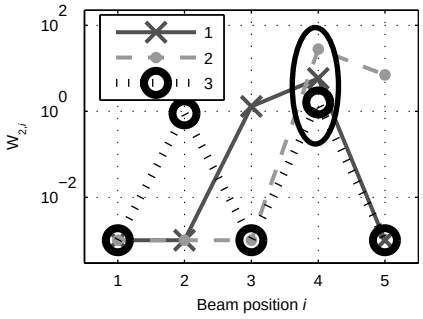

Fig. 10. Optimization results of W_2 for add-on mass of 20 % beam mass in position 4 and **(1)** excitation in position 2, reference measurement in position 5, measurement for PIO in position 3. For **(2)** exc. in pos. 2, ref. meas. in pos. 3, meas. for PIO in pos. 5, and for **(3)** exc. in pos. 3, ref. meas. in pos. 5, meas. for PIO in pos. 2.

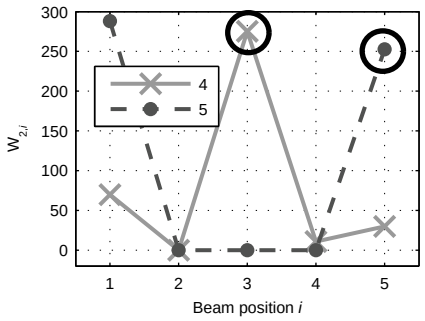

Fig. 11. Optimization results of W_2 for add-on mass of **(4)** 15 % beam mass in position 3 and excitation in position 3, measurements in positions 2 and 5 (PIO and reference), and for **(5)** add-on mass of 10 % beam mass in position 5 and excitation in position 2, measurements in positions 1 and 3 (PIO and reference).

was only possible if two displacement measurements are used as PIO inputs, one corresponding optimization result is shown in Fig. 11. Below 15 % beam mass change no localization was possible.

Figure 11 shows an example for an add-on mass of about 10 % beam mass in position 5. The beam was excited in position 2 and both displacement measurements in the positions 1 and 3 were used as PIO inputs as well as for the optimization. But the largest element of W_2 denotes position 1 as the add-on mass location, the value for position 5 is lower. In this case the localization fails.

B. Localization of a beam crack

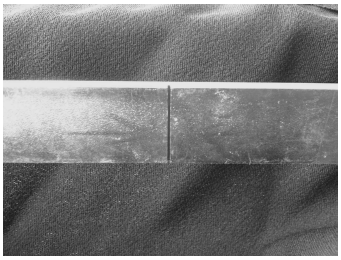

Fig. 12. Beam crack simulated by a saw cut of about 1/3 beam-thickness in the third beam segment.

A crack is simulated by a saw cut of about 1/3 beam-thickness in the middle of the third beam segment, see Fig. 12. A successful localization of the saw cut is illustrated in Fig. 13. Its three curves represent different optimization results of the $W_{2,i}$-components of which each represents a torque acting on the corresponding beam segment. In the given case the torque at the third segment is weighted the most, correctly indicating the saw cut in the third beam segment. For the localization (2) only a single measurement at position 2 is used. That one drives the PIO, which estimates the displacement at position 2 itself. Estimation and measurement are compared, the error is used to tune the $W_{2,i}$-components as illustrated in Fig. 3. Analogously only the measurement in position 3 is used for the successful localization (3). For (1) both measurements are combined, both are used to feed the PIO and for reference. The larger amount of information leads to a very clear localization of the saw cut – the torques related to the beam segments 2, 4 and 5 are about 0, but the torque which corresponds to segment 3 is strongly weighted with about 16000.

Of course the localization results depend on measurement positions and excitation points – controllability and observability aspects have to be taken into account. But just to have a fully observable system from a mathematical point of view is not sufficient. It is important that the modes which are strongly affected by a crack can be measured and stimulated significantly at the chosen positions. Figure 14 illustrates an example for a failed localization. The measurements in positions 4 and 5 are used for the PIO as well as for reference. Obviously the crack is not located – the torques for the segments 3, 4, and 5 are weighted similar.

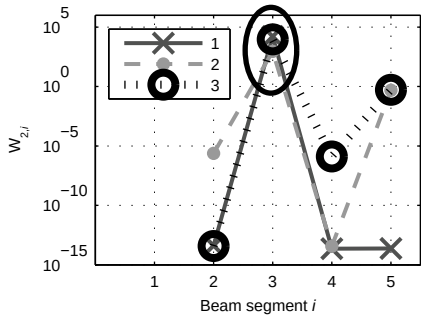

Fig. 13. Optimization results of W_2 for crack of about 1/3 beam-thickness in the middle between beam positions 2 and 3, in segment 3 (ellipse). The beam is excited in position 1. (1) Displacement measurements in positions 2 and 3 are used for PIO as well as for reference. (2) Only measurement in position 2 is used for PIO and for reference. (3) Only measurement in position 3 is used for PIO and for reference.

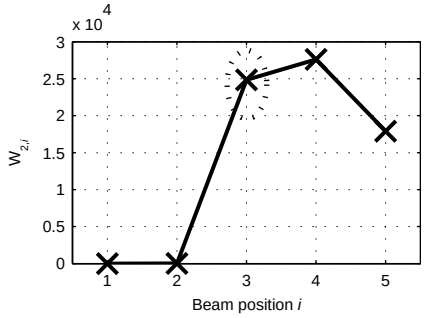

Fig. 14. Optimization results of W_2 for crack of about 1/3 beam-thickness in the middle between beam positions 2 and 3, in segment 3 (ellipse). Excitation in position 2, measurements in positions 4 and 5 (PIO and reference).

VI. Integrating Diagnosis and Control into Reliability-Based Concepts Realizing Safe Structures

The *Safety and Reliability Control Engineering* (SRCE) concept provides a framework and strategy to calculate the actual reliability of a system under operation including the load history. The online-calculated reliability depends on the actual load and the load history of the system. The determination of the individual actual reliability of a system may be used for the purpose of condition-based maintenance or condition monitoring. By the knowledge of the correlation between the

load and the reliability characteristics it may be possible to change the load with objective to achieve a given maximum amount of utilization before a critical probability of failure appears.

The integration of diagnosis and prognosis into a reliability-based approach like the SRCE-concept consists of two paths combined to realize a new quality of systems safety by supervision and control. Based on real or virtual sensors information are taken from the system and used for calculation of online reliability characteristics (SRCE-approach). Core of the SRCE-approach is the use of related damage laws and damage calculation relations. This closes the loop from virtual sensors to reliability and damage and allows specific system states online evaluation.

The utilization of the maximum life cycle of a technical system or component is getting more and more important. Because of economical or safety reasons, operators have to use technical components up to the maximum possible life. This demand can only be achieved, if knowledge about the actual state of the components concerning failure and the knowledge about how to change the operating mode to expand life time is given. There are several reasons to expand the life of a technical system or component which will probably fail if the actual operation mode continues. One reason may be the achievement of a special time at which maintenance measures are feasible, e. g. if the access to the system is given only at this time or if maintenance costs are lower, if they are realized at this time (nighttime, mission to be fulfilled, holiday season etc.). Another reason may be that systems with no failsafe state like aircrafts in flight have to reach a safe state which implies an expansion of the maximum utilization if the expected maximum utilization is below the desired utilization. Also for unmanned space vehicles like autonomous submarines the completion of a defined mission even in case of excessive loads may be very important.

This aspects are important if failures or structural changes inside a structure or system occur. In this case the related effects form the changes has to be taken into account: the definition of related utilizable life time, hazard rates etc. can be used to control the mission by effecting the related reliability characteristics .

The *Safety and Reliability Control Engineering* concept (SRCE-concept) was explained in detail in [4], [7], [9]. In [7], [10] the idea is extended by introducing a model-predictive control approach, calculating the reliability characteristics online for assumed upcoming load trajectories. This allows an online optimization of the operating parameters and therefore realizes a reliability-oriented loop between online-'measured' system state, operating parameters and also maintainance approaches.

A general sketch of the SRCE-concept is shown in Fig. 15. To apply the SRCE-concept to a real system that is used with individual operating parameters the following information has to be given / requirements has to be fulfilled.

- Signals that represent the stress of the system or the relevant component have to be present. Stress in this case means the response of a component to the applied loads. These signals can be getting by suitable sensor devices or by virtual sensors-based on model-based approaches.
- A valid damage process and damage accumulation law for the considered component, including material, design, and environment has to be known.
- Another important point is the availability of an empirical database that describes the correlation between the applied stress and the expected maximum utilization. The latter can be given in mileage, flying hours, cycles or the like, depending on the system.

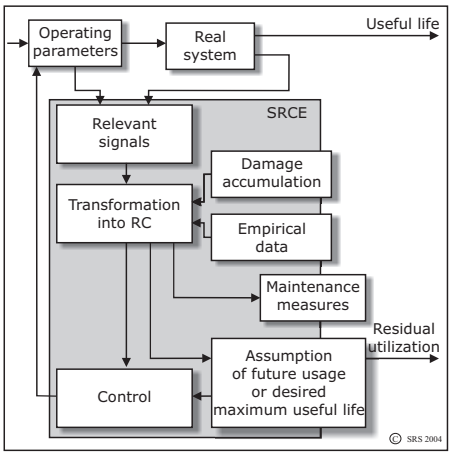

Fig. 15. Principle structure of the SRCE-concept.

With this information the signals can be transformed in a stress depending reliability characteristic RC that can be used. The knowledge of the connection between the operation mode, the stress, and the failure behavior can be used inversely to control the maximum utilization [7]. The empirical database can be represented with S-U-R diagrams and adding an additional abscissa for the damage like shown in Fig. 16. All assumptions for the validity of such a diagram and a way how to append the damage axis are given in [8].

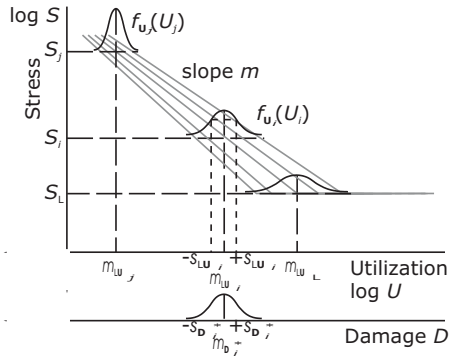

Fig. 16. S-U-R diagram with additional damage axis.

The use of this approach results in a probability of failure for the system that is defined as

$$Pr\{D_i^* \leq D_i\}. \tag{16}$$

With the assumptions that

- the maximum utilization U is lognormal distributed,

- the critical (maximum) damage D_i^* is normal distributed, and
- the damage accumulation law of Palmgren-Miner is suitable the above introduced eq. can be solved using

$$F_{D_i^*(D_i)} = \Phi\left(\frac{\mu_{D_i} - \mu_{D_i^*}}{\sqrt{(\sigma_{D_i^*}^2 + \sigma_{D_i}^2)}}\right). \quad (17)$$

This RC can be graphically described as the area of overlapping between the probability density function (PDF) of the accumulated damage D, representing the stress history and the PDF of the critical damage D_i^*, representing the actual stress (Fig. 17).

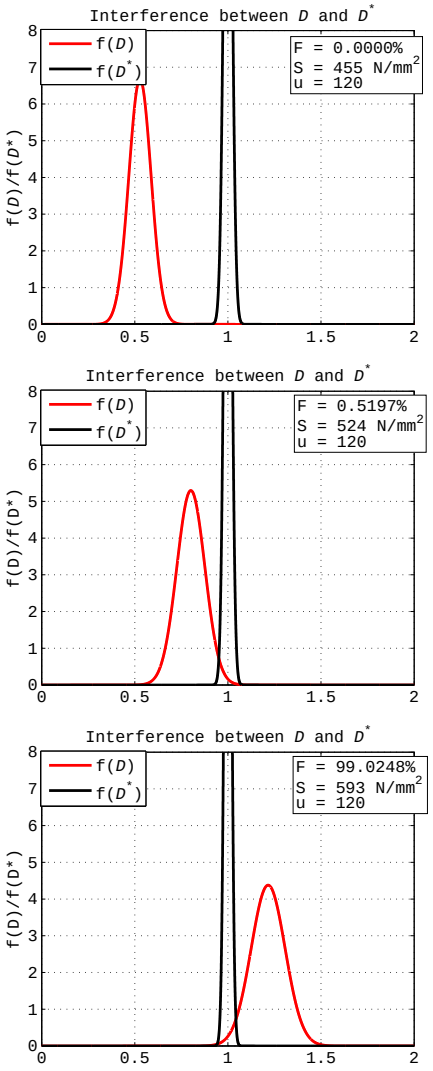

Fig. 17. Area of overlapping different stress levels $S1, S2, S3$.

The overlapping of the PDFs and with it the probability of failure (POF) is given in Fig. 17 for different stress levels $S1 < S2 < S3$, whereby $S1$ is shown in the upper figure, $S2$ in the mid, and $S3$ in the bottom figure. The plots show the situation at 120 usages. The gray/red line indicates the PDF of the accumulated damage while the black line represents the PDF of the critical damage. The empirical database are taken from the experiments of [6], working here just as an example $S1 = 455\,N/mm^2, S2 = 524\,N/mm^2, S3 = 593\,N/mm^2$. It can be seen, that the POF at the same usages increases from below 0.0000 to 99.0248 (percent) with increasing stresses.

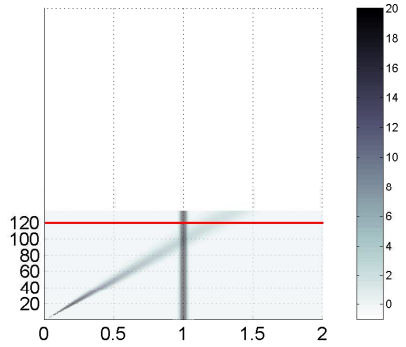

Fig. 18. Example 3D-representation of the progression of the area of overlapping.

In Fig. 18 as an example the progression of the PDFs for the introduced stress level is given in a 3D-plot up to a POF of 0.9998. The third dimension (PDF) is given grayscaled. The straight line indicates the point at $u = 120$ (usage number). The effect that the POF depends on the actual applied stress, and is also illustrated in Fig. 19.

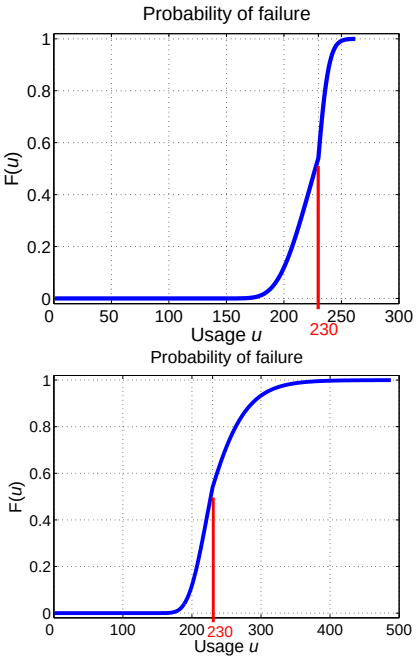

Fig. 19. Progression of POF for different changing stress levels.

Both diagrams show the POF for a constant stress of $S1$ up to the usage $u = 230$. In the left diagram the stress increases at $u = 231$ up to S of $662\,N/mm^2$. The result is a maximum utilization of 262 usages (Break condition is POF = 0.9998). In the right diagram the stress is reduced to $S = 386\,N/mm^2$. This results in a maximum utilization of 488 usages; this is

approximate 1.9-fold of the one of the left case and 1.3-fold of the one with the unchanged stress level.

To demonstrate idea and the potential of SRCE-concept the following scenario is discussed: The real development of the RC differs from the expected development in that case, that the $RC = RC_u$ for a given point of utilization is greater than expected (for a smaller the better RC). In other words, the calculated RC should normally be achieved at a point of utilization u_2 that is beyond the actual utilization u_2. The cause is unexpected high loads and with it increased stresses. If the use of the system continues with these loads, a maximum utilization of u_{max1} can be achieved. With the assumption, that the stress is constant, the expected maximum utilization is u_{max2} and can be calculated by

$$F_{D_i^*(D_i)} = \Phi(\frac{\mu_{D_i} - \mu_{D_i^*}}{\sqrt{(\sigma^2_{D_i^*} + \sigma^2_{D_i})}}) = \Phi(\xi), \tag{18}$$

where μ_{D_i} can be represented by u_{max2,μ_d} and σ_{D_i} by u_{max2,σ_d}. Here μ_d and σ_d denote the parameters of the distribution of the damage friction, μ_d^* and σ_d^* denote the parameters of the distribution of the critical damage. The parameters F_c and ξ denote the critical POF $= RC_c$ and the corresponding quantile of the standard normal distribution. The inversion for u_{max2} is given by

$$\begin{aligned} u_{max2} &= -\frac{\mu_d \mu_D}{\sigma_d^2 \xi^2 - \mu_d^2} \\ &+ \frac{sgn(F_c - 0.5)\sqrt{-\xi^2 \sigma_d^2 \sigma_{D*}^2 + \mu_{D^*}^2 \sigma_d^2 + \mu_d^2 \sigma_{D^2}^2 \xi}}{\sigma_d^2 \xi^2 - \mu_d^2} \end{aligned} \tag{19}$$

The question is how to change the stress level to achieve the desired maximum utilization u_{max2}? The solution can be given using the real solution of the polynom

$$\xi = a_6 s^6 + a_5 s^5 + a_4 s^4 + a_3 s^3 + a_2 s^2 + a_1 s + a_0 \tag{20}$$

as approximation of the complex equation resulting from inverting the expression developed before $u_{max2} = f(\mu_d, \mu_D, F_c, \xi, \mu_{D^*}, \sigma_d, \sigma_{D^*})$ given end developed explicitely in [9]. The developed solution requires the actual amount of the utilization u_i, u_{max} as u_{max2} as well as parameters from the linear equations for μ_u and σ_u in the S-U-R diagram. This equations has to be solved for the stress level S to get the solution. Due to the not available exact solution, the introduced approximation, which is valid in this calculation example for stress levels S = [345,827] N/mm^2 can be used. The reduction of the stress can only be achieved by reducing the load and hence by changing the operation parameters. Generally this results in an operation mode of the system with a loss of performance, but not necessarily with a general loss of functionality. To guarantee a minimum degree of performance the stress level can have a lower limit. If the solution results to a stress below this limit, the application is not feasible. The question arises, what can be the possible maximum utilization u_{max} when the minimum stress level (lower stress limit) is applied? Also this solution can be derived from the approximation introduced before, with S as the minimal stress S_{min} and the related equation to be solved for u_{max}. As an approximation here an polynomal approach of 7th order between u_{max} and ξ is used as

$$\begin{aligned} \xi &= a_7 u_{max}^7 + a_6 u_{max}^6 + a_5 u_{max}^5 \\ &+ a_4 u_{max}^4 + a_3 u_{max}^3 + a_2 u_{max}^2 + a_1 u_{max} + a_0 \end{aligned} \tag{21}$$

This approximation is valid in a certain interval, in this case for u_{max} = [10,800]. The real solution results as the maximum utilization u_{max} that can be achieved under the given constraints.

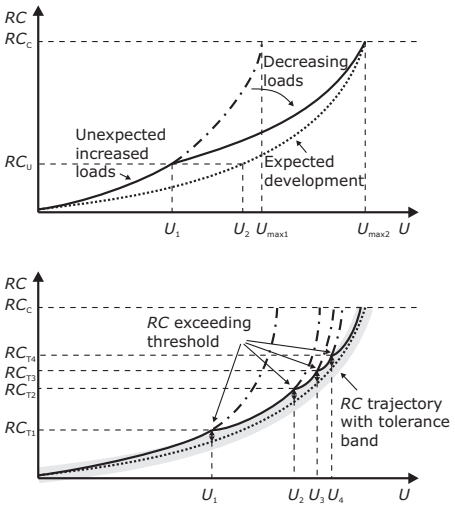

Fig. 20. Progression of POF for different changing stress levels 2: Illustration of the example.

The illustrated example should only clarify the special aspect of the consideration of the utilization extension, details are given in the previously mentioned articles [7], [8], [9]. In this context a possible control task is to control systems functionality from a probabilistic point. If the systems harzard rate is detected (by calculation) as not acceptable (larger than a given scalar number) the systems operations mode has to be changed (typically by reducing the stress level/by reducing the load applied to the system).

This is what RC will be achieved if the stress is higher than expected and no change of the operation mode will be applied? Is it really necessary to change the operating parameters and to reduce the performance? As answer also the introduced strategy as solution for $u_{max} = u_{max1}$ is illustrated, cf. Fig. 20. The calculated value is the F_c-quantile of the standard normal distribution which describes the POF for the given assumptions as introduced. A short example is given to demonstrate the given explanations and illustrated graphically in Fig. 20. A system shall be run with a desired stress of S_d = 455 N/mm^2. The maximum utilization for a critical POF of F_c = 0.05 can be calculated as u_{max} = 190. The real stress acting on the system is $S_r = 462\,N/mm^2$ that results in u_{max} = 183. If the system is going on to operate under stress S_r, the POF at u = 190 will be F = 0.09 which is nearly two times F_c. Let assume that the deviation of the RC from the desired progression can only be detected if a significant divergence of ΔF = 0.005 is given. This is the case for u= 171. To achieve the desired maximum utilization,

the stress has at least to be decreased to S_r = 386 N/mm^2. With the assumption, that the system may even operate with a reduced operation mode resulting in stress of 345 N/mm^2 the calculated stress S_r can be applied.

As briefly illustrated, the potential of the concept can be summarized in two main aspects. The first is the determination of a RC based on the individual usage and usage history. This RC gives more precious prediction of failures of a system which may be important as a support for shut-down decisions or as an assessment basis of future usages. The second is the calculation of the maximum stress which has to be applied to achieve a desired amount of utilization. This offers the possibility to extend the utilization for several reasons (safety, economy, or organization) by implementing a limp home mode with reduced performance. The effect can be used for optimization of measures like repair or replacement or for a quantification of the feasibility of future usages.

VII. Conclusions and outlook

The development of new elastic mechanical structures especially in the context of multifunctional structures leads to new functionalities, but also to new dependabilities. Therefore the combination of observer, this means model-based techniques like the proposed PI-Observer, and integrated sensor/acuator hardware like PZT-patches may lead to highly integrated and self-monitoring/self-sensing systems.

The proposed (M)PI-Observer allows the estimation of internal and external unknown effects. This basic ability is extended by an numerical optimization approach for fault localization purposes. The key advantage of the proposed approach is, that only few measurements are necessary and that the observer can be used for the whole range of diagnosis : Detection, estimation and localization. It provides the system states as well as estimations of additive unknown effects/inputs, representing internal or external forces or torques acting on the observed structure. These features allow for the PIO to serve as virtual sensor device in order to replace physical sensors or to deliver data for immeasurable states and locations where no physical sensor is available or applicable.

The MPIO in combination with the experimentally derived beam model is tested for localization purposes. The MPIO is limited to the first three beam modes due to significant resolution restrictions of the used laser sensors. The localization approach suffers under this unwanted restriction because the number of ascertainable modes strongly determines the amount of information usable to locate system changes. Under the given conditions, mass changes for at least 15% of the test beam can be located. Additionally, the approach has been tested for the detection of a beam crack, simulated by a saw cut of about 1/3 beam-thickness. For specific combinations of measurement and excitation positions the localization is successful and significant.

The SRCE-concept introduced and developed at the Chair of Dynamics and Control allows the monitoring of the ageing process of new sensory and actuation devices. Together with the PIO-based diagnosis approach it can be applied to ensure safe system operation. The next step will be the full hardware integration of the techniques within a structure. Other work will care about the integration of acceleration measurements within this new structural health monitoring (SHM) concept for adaptronic structures.

References

[1] Heidtmann, F. and Söeffker, D. (2008). *Numerical Optimizations in Observer-Based Monitoring of Elastic Mechanical Systems*. Proc. International Conference on Prognostics and Health Management PHM2008, Denver, Colorado, USA, 8 pages.

[2] Patton, R.J; Frank, P.M.; Clark, R.N. (2000). *Issues in fault detection for dynamic systems*. Springer: London.

[3] Söffker, D. (1995). *A New Model-based Tool for Failure Detection and Isolation in Machine- and Rotordynamics*. ASME DE-Vol. 83-2, pp. 233-242.

[4] Söffker, D. (2000). *Zur Online-Bestimmung von Zuverlässigkeits- und Nutzungskenngrössen innerhalb des SRCE-Konzeptes*. at-Automatisierungstechnik 48, pp. 383-391.

[5] Söffker, D.; Kashi, K.; Wolters, K. (2005). *Integration of Reliability Concepts, Diagnosis, and Control to Realize Safe Systems*. Proc. of ESREL 2005, Poland, 08.2005.

[6] Corten, H.T.; Dolan, T.J. (1956). *Cumulative Fatique Damage*. in: Proceedings Int. Conf. on Fatigue of Metals, IME, ASME.

[7] Wolters, K.; Söffker, D. (2003). *Control of damage dependent online reliability characterictics to extend system utilization* . in: Structural Health Monitoring 2003, Chang, F.K. (Ed.), Stanford, pp. 796-804.

[8] Wolters, K.; Söffker, D. (2004). *Improving systems availability by combining reliability and control engineering techniques* . in: ESREL, Proc. 2nd European Workshop of Structural Health Monitoring 2004, pp. 711-720.

[9] Wolters, K.; Söffker, D. (2005). *The potential of the Safety and Reliability Control Engineering Concept as framework for reliability based utilization strategies* . in: Structural Health Monitoring 2005, Chang, F.K. (Ed.), Stanford, pp. 1353-1360.

[10] Wolters, K. (2008). *Formalismen, Simulation und Potenziale eines nutzungsdaueroptimierenden Zuverlässigkeitskonzepts* . Dr.-Ing. Dissertation, University of Duisburg-Essen.

[11] M. I. Friswell and J. E. Mottershead, *Finite Element Model Updating in Structural Dynamics*, ser. Solid mechanics and its applications. Dordrecht: Kluwer, 1996, vol. 38.

[12] H. H. Müller-Slany, "Model Updating a Multicriteria Optimization Process in Mechanics," in *Mechanics of the 21st Century. Proc. of the 21st International Congress of Theoretical and Applied Mechanics, Aug. 15–21, 2004, Warsaw, Poland*, W. Gutkowski and T. A. Kowalewski, Eds. Dordrecht: Springer, 2005.

[13] D. Bernal, "Modal Scaling from Known Mass Perturbations," *JOURNAL OF ENGINEERING MECHANICS-ASCE*, vol. 130, no. 9, pp. 1083–1088, Sep. 2004.

[14] R. Brincker, P. Andersen, and S. Gade, "Mode Shape Scaling by Mass Changes," in *Proc. of the INTER-NOISE 2003 Conference*, Jeju, Korea, Aug. 25–28 2003.

[15] E. Parloo, P. Verboven, P. Cuillame, and M. v. Overmeire, "Sensitivity-Based Mass-Normalization of Mode Shape Estimates from Output-Only Data," in *Proc. of the International Conference on Structural System Identification*, Kassel, Germany, 2001, pp. 627–636.

[16] F. Heidtmann and D. Söffker, "Experimental-Modeling-Based Observer Approach for the Analysis of Structural Changes in Elastic Mechanical Systems," in *Proc. of the 9th International Conference on Motion and Vibration Control MOVIC 2008*, Munich, Germany, Sep. 15–18 2008.

[17] S. Beale and B. Shafai, "Robust control design with a proportional integral observer," *Int. J. Control*, vol. 50, pp. 97–111, 1989.

[18] P. C. Müller, "Control of Nonlinear System by Applying Disturbance Rejection Control Technique," in *Proc. IEE International Conference CONTROL 88, Institution of Electrical Egineers, London*, 1988, pp. 734–737.

[19] H. H. Niemann, J. Stroustrup, B. Shafai, and S. Beale, "LTR Design of Proportional Integral Observers," *Int. J. Rob. and Nonl. Control*, vol. 5, pp. 671–693, 1995.

[20] D. Söffker, T. J. Yu, and P. C. Müller, "State Estimation of Dynamical Systems with Nonlinearities by using Proportional-Integral Observer," *Int. J. Systems Science*, vol. 26, no. 9, pp. 1571–1582, 1995.

[21] D. Söffker, "New Results of the Development and Application of Robust Observers to Elastic Mechanical Structures," in *IUTAM Symposium on Vibration control of Nonlinear Mechanism and Structures, July 18–11, 2005, Munich, Germany*, ser. Solid Mechanics and its Applications, H. Ulbrich and W. Günthner, Eds., vol. 130. Springer, 2005, pp. 319–330.

[22] I. Krajcin and D. Söffker, "Diagnosis and Control of 3D Elastic Mechanical Structures," in *Proc. 12th International Symp., Smart Structures and Materials: Smart Structures and Integrated Systems*, San Diego, California, USA, March 6–10 2005, pp. 100–113.

[23] I. Krajcin, *Einsatz des PI-Beobachters zur modellbasierten Diagnose und Regelung elastischer mechanischer Strukturen*, ser. Berichte aus der Steuerungs- und Regelungstechnik. Aachen: Shaker, 2006.

[24] D. Söffker, J. Bajkowski, and P. C. Müller, "Detection of cracks in turborotors – a new observer based method," *ASME J. Dyn. Systems, Meas. and Control*, vol. 115, pp. 518–524, 1993.

[25] ——, "Modified PIO Design for Robust Unknown Input Estimation," in *Proc. 19th ASME DETC Biennial Conference on Mechanical Vibration and Noise, Sep. 2–6, 2003, Chicago, Illinois, USA*, ser. Proc. of the 2003 Design Engineering Technical Conferences, vol. 5. New York, N.Y.: American Society of Mechanical Engineers, 2003, pp. 1459–1464.

[26] D. Söffker, J. Bajkowski, and P. C. Müller, "Analysis and Detection of the Cracked Rotor," *ZAMM*, vol. 73, pp. 87–91, 1992.